

Crystal structure of (*E*)-doxepin hydrochloride, C₁₉H₂₂NOClJerry Hong,¹ Joseph T. Golab,¹ James A. Kaduk^{2,3,a)} Amy M. Gindhart,⁴ and Thomas N. Blanton⁴¹Illinois Mathematics and Science Academy, 1500 Sullivan Rd., Aurora, Illinois 60506-1000, USA²Illinois Institute of Technology, 3101 S. Dearborn St., Chicago, Illinois 60616, USA³North Central College, 131 S. Loomis St., Naperville, Illinois 60540, USA⁴ICDD, 12 Campus Blvd., Newtown Square, Pennsylvania 19073-3273, USA

(Received 18 November 2020; accepted 16 December 2020)

The crystal structure of (*E*)-doxepin hydrochloride has been solved and refined using synchrotron X-ray powder diffraction data, and optimized using density functional techniques. (*E*)-doxepin hydrochloride crystallizes in space group $P2_1/a$ (#14) with $a = 13.78488(7)$, $b = 8.96141(7)$, $c = 14.30886(9)$ Å, $\beta = 96.5409(5)^\circ$, $V = 1756.097(12)$ Å³, and $Z = 4$. There is a strong discrete hydrogen bond between the protonated nitrogen atom and the chloride anion. There are six C–H...Cl hydrogen bonds between the methyl groups and the chloride, as well as additional hydrogen bonds from methylene groups and the vinyl proton. The hydrogen bonds are important in determining the solid-state conformation of the cation. The compound is essentially isostructural to amitriptyline hydrochloride. The powder pattern is included in the Powder Diffraction File™ as entry 00-066-1613. © The Author (s), 2021. Published by Cambridge University Press on behalf of International Centre for Diffraction Data. [doi:10.1017/S0885715621000063]

Key words: doxepin, (*E*)-doxepin hydrochloride, powder diffraction, Rietveld refinement, density functional theory

I. INTRODUCTION

Doxepin hydrochloride (brand names include Adapin, Aponal, Curatin, Quintaxon, and Sinequan) is a tricyclic antidepressant (TCA). Its chemical structure features a tricyclic ring system accompanied by an alkyl amine substituent. TCAs such as doxepin are potent inhibitors of serotonin and norepinephrine reuptake. Other medicinal uses for doxepin hydrochloride include treating anxiety and insomnia, and as a topical application for treating skin dermatitis. Both (*E*)- and (*Z*)-isomers of doxepin hydrochloride are known, and available commercially. (*Z*)-doxepin corresponds to cidoxepin. The IUPAC name of doxepin hydrochloride is (3*E*)-3-(6H-benzo[*c*] [1]benzoxepin-11-ylidene)-*N,N*-dimethylpropan-1-amine hydrochloride. The CAS Registry number for the mixed isomers of doxepin HCl is 1229-29-4, and for the (*E*)-isomer is 4698-39-9. A two-dimensional molecular diagram for the doxepin cation is shown in Figure 1.

Low-precision powder patterns of doxepin hydrochloride are contained in the ICDD® Powder Diffraction File (PDF®) as entries 00-029-1697 (Haga, 1979) and 00-034-1704 (DeCamp, 1982). Higher quality patterns of *trans*-doxepin hydrochloride and *cis*-doxepin hydrochloride are included as entries 00-034-1706 (DeCamp, 1982) and 00-051-1920 (Jin, 2001), respectively. However, none of these entries contains crystal structure data. Polymorphism in doxepin hydrochloride has been studied by Panda (2011).

This work was carried out as part of a project (Kaduk *et al.*, 2014) to determine the crystal structures of large-volume commercial pharmaceuticals, and include high-quality

powder diffraction data for these pharmaceuticals in the Powder Diffraction File (Gates-Rector and Blanton, 2019).

II. EXPERIMENTAL

Doxepin hydrochloride was a commercial reagent, purchased from United States Pharmacopeial Convention (USP) (Lot # J0M472), and was used as-received. It was unknown if the sample was a mixture or single isomer. The white powder was packed into a 1.5-mm diameter Kapton capillary and rotated during the measurement at ~50 Hz. The powder pattern was measured at 295 K at beam line 11-BM (Lee *et al.*, 2008; Wang *et al.*, 2008) of the Advanced Photon Source at Argonne National Laboratory using a wavelength of

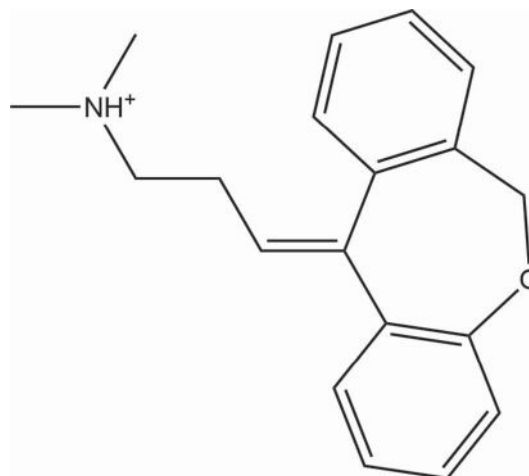


Figure 1. The molecular structure of the (*E*)-doxepin cation.

^{a)} Author to whom correspondence should be addressed. Electronic mail: kaduk@polycrystallography.com

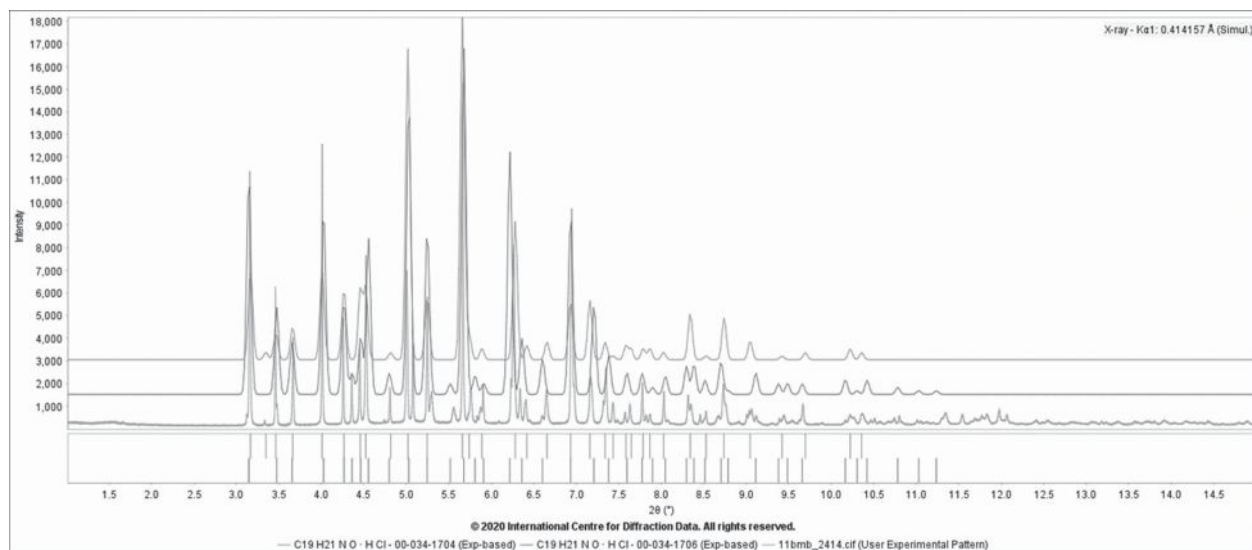


Figure 2. Comparison of the synchrotron powder pattern (green) of doxepin hydrochloride to the 2θ , intensity data for the two reported *trans*-doxepin PDF entries (00-034-1704 (red), 00-034-1706 (blue)).

0.414157 Å from 0.5° to 50° 2θ with a step size of 0.001° and a counting time of 0.1 s step^{-1} . The observed diffraction pattern was found to correspond to *trans*-doxepin hydrochloride (Figure 2). The pattern was indexed on a primitive monoclinic unit cell with $a = 13.78472$, $b = 8.96160$, $c = 14.30891$ Å, $\beta = 96.540^\circ$, $V = 1756.121$ Å³, and $Z = 4$ using N-TREOR (Altomare *et al.*, 2013). Analysis of the systematic absences using EXPO2014 (Altomare *et al.*, 2013) suggested the space group $P2_1/a$, which was confirmed by successful solution and refinement of the structure. A reduced cell search in the Cambridge Structural Database (Groom *et al.*, 2016) yielded 7 hits, among which was amitriptyline hydrochloride (Klein *et al.*, 1994; YOVZEO). This molecule has the same connectivity as doxepin, but without the oxygen atom in the

central ring. The structure was solved by direct methods, including the COVMAP option.

Rietveld refinement for (*E*)-doxepin HCl was carried out using GSAS-II (Toby and Von Dreele, 2013). Only the 1.6 – 25.0° portion of the pattern was included in the refinement ($d_{\min} = 0.956$ Å). All non-H bond distances and angles were subjected to restraints, based on a Mercury/Mogul Geometry Check (Bruno *et al.*, 2004; Sykes *et al.*, 2011) of the molecule. The results were exported to a .csv file. The Mogul average and standard deviation for each quantity were used as the restraint parameters and were incorporated using the new feature Restraints/Edit Restraints/Add MOGUL Restraints, which reads the bond distance and angle restraints from the .csv file. The restraints contributed 3.8% to the final χ^2 . The

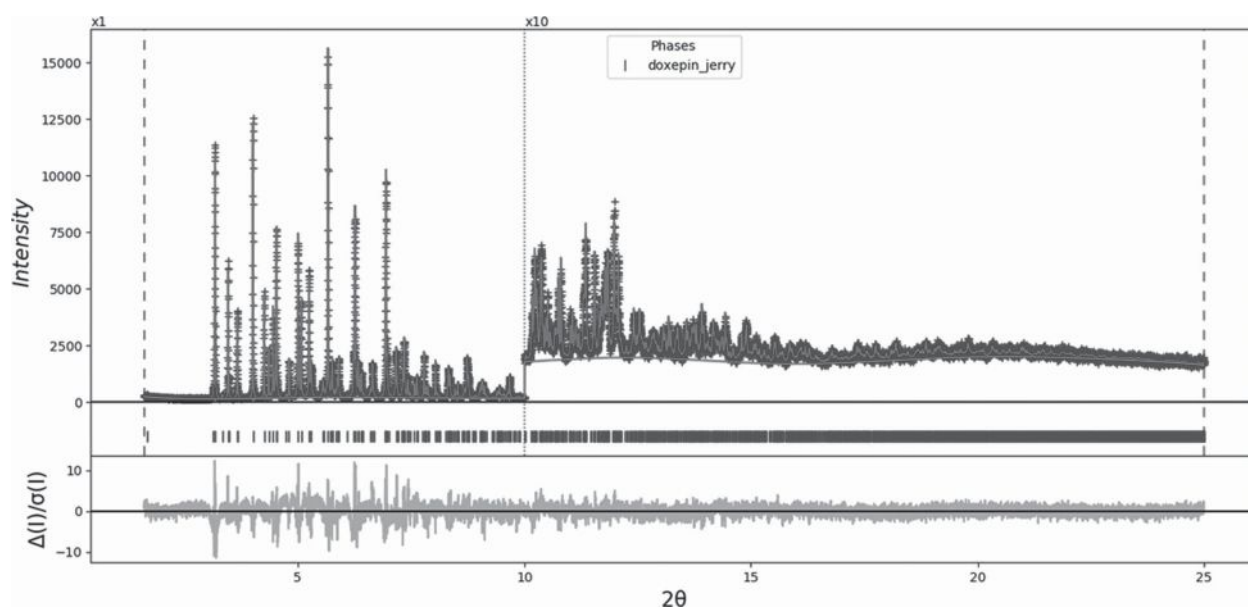
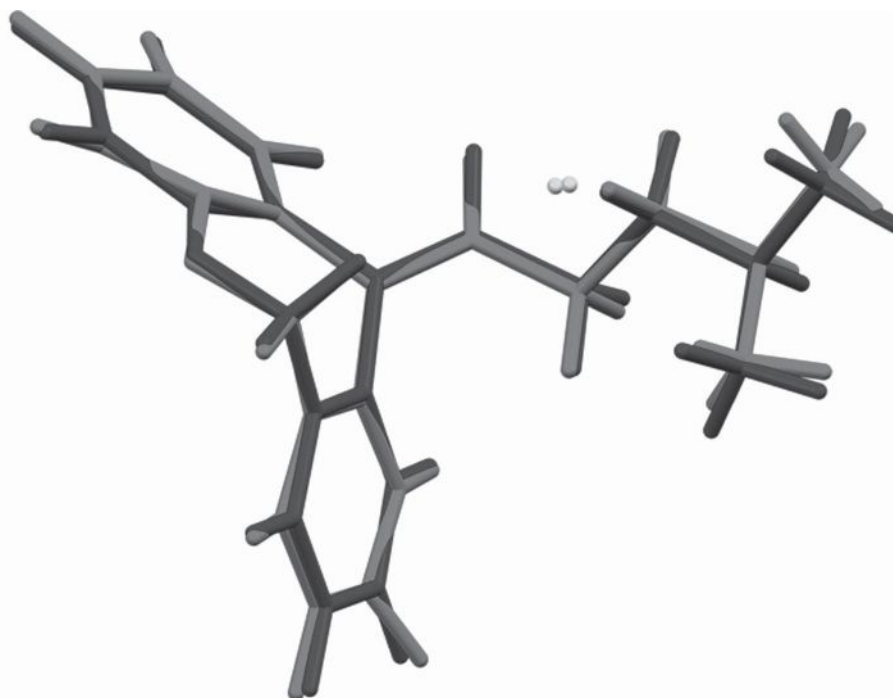


Figure 3. The Rietveld plot for the refinement of doxepin hydrochloride. The blue crosses represent the observed data points, and the green line is the calculated pattern. The cyan curve is the normalized error plot. The vertical scale has been multiplied by a factor of $10\times$ for $2\theta > 10.0^\circ$.



Rms delta = 0.122, max = 0.217 at methyl C35

Figure 4. Comparison of the Rietveld-refined (red) and VASP-optimized (blue) structures of doxepin hydrochloride. The rms Cartesian displacement is 0.122 Å.

hydrogen atoms were included in calculated positions, which were recalculated during the refinement using Materials Studio (Dassault, 2019). The U_{iso} for each hydrogen atom was constrained to be $1.3\times$ that of the heavy atom to which it is attached. The background was modeled using a 4-term shifted Chebyshev polynomial, and an 8-term diffuse scattering function to model the Kapton capillary and any amorphous component.

The final refinement of 104 variables using 23 402 observations and 54 restraints yielded the residuals $R_{\text{wp}} = 0.0832$ and $\text{GOF} = 1.59$. The largest peak (0.17 Å from C143) and hole (1.59 Å from N34) in the difference Fourier map were 0.29 and $-0.17(4) e\text{Å}^{-3}$, respectively. The Rietveld plot is included in Figure 3. The largest errors in the fit are in the shapes of some of the strong low-angle peaks.

A density functional geometry optimization was carried out using CRYSTAL14 (Dovesi *et al.*, 2014). The basis sets for the H, C, N, and O atoms were those of Gatti *et al.* (1994), and the basis set for Cl was that of Peintinger *et al.* (2013). The calculation was run on eight 2.1 GHz Xeon cores (each with 6 GB RAM) of a 304-core Dell Linux cluster at IIT, using 8 k -points and the B3LYP functional, and took ~ 52 h.

III. RESULTS AND DISCUSSION

The refined atom coordinates of (*E*)-doxepin hydrochloride and the coordinates from the density functional theory (DFT) optimization are reported in the CIFs attached in the Supplementary Material. The root-mean-square (rms) Cartesian displacement of the non-hydrogen atoms in the Rietveld-refined and DFT-optimized structures is 0.122 Å

(Figure 4). The maximum difference is at the methyl group C35. The agreement between the refined and optimized structures is excellent and provides evidence that the experimental structure is correct (van de Streek and Neumann, 2014). This discussion concentrates on the CRYSTAL-optimized structure. The asymmetric unit (with atom numbering) is illustrated in Figure 5, and the crystal structure is presented in Figure 6.

All of the bond distances, bond angles, and torsion angles fall within the normal ranges indicated by a Mercury/Mogul Geometry check (Macrae *et al.*, 2020). The N–H \cdots Cl hydrogen bonds lie along the a -axis. As noted below, C–H \cdots Cl hydrogen bonds also occur, and lead to columns of hydrogen bonds along this axis. The central ring of the cation is bent, leading to a “butterfly” shape of the fused ring system. The structure of the doxepin cation is essentially identical with the cation in YOYZEO (changing the O14 to a carbon and inverting one of the structures). The rms Cartesian displacement is only 0.084 Å (Figure 7), and the maximum displacement is 0.129 Å. The YOYZEO structure could have been used as an initial model for the Rietveld refinement, if we had not already solved the structure by direct methods.

Quantum chemical geometry optimizations (DFT/ B3LYP/6-31G*/water) of the (*E*)-doxepin cation using Spartan '18 (Wavefunction, 2018) indicated that the observed conformation is $2.9 \text{ kcal mol}^{-1}$ higher in energy than the local minimum, and thus that the cation is in a low-energy conformation. The minimum-energy conformation (molecular mechanics) is much more compact and distorted, with the two aromatic rings parallel to each other and the side chain also folded toward the ring system. Intermolecular interactions

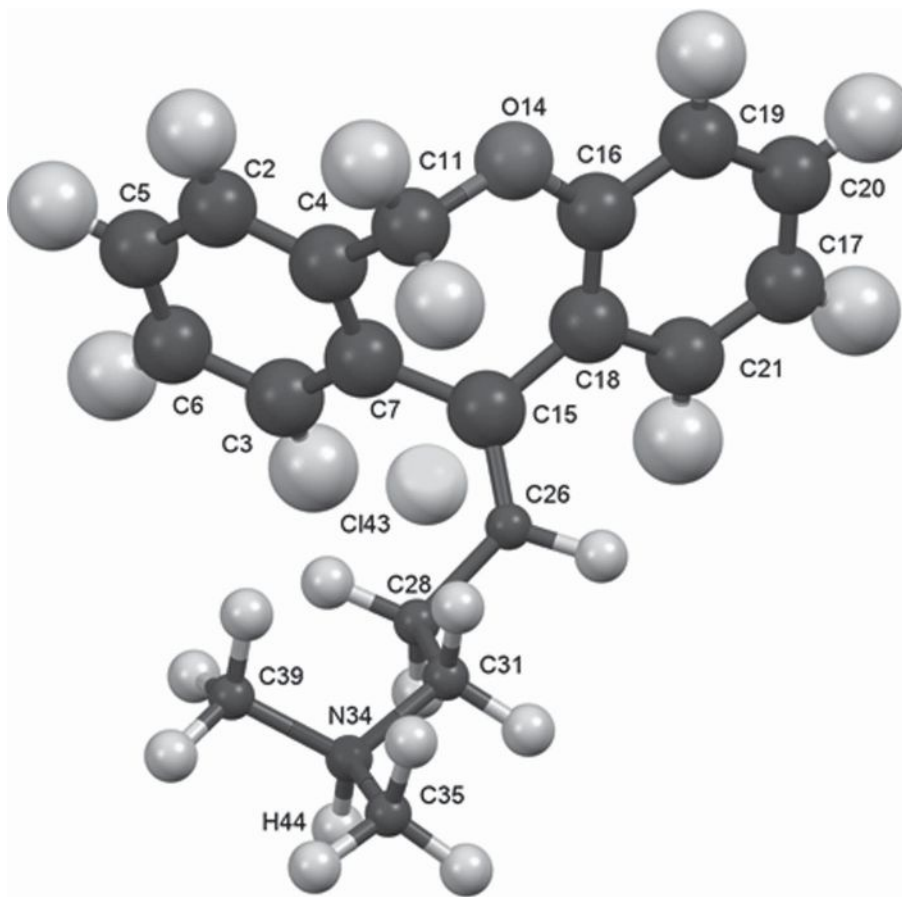


Figure 5. The asymmetric unit of doxepin hydrochloride, with the atom numbering. The atoms are represented by 50% probability spheroids/ellipsoids.

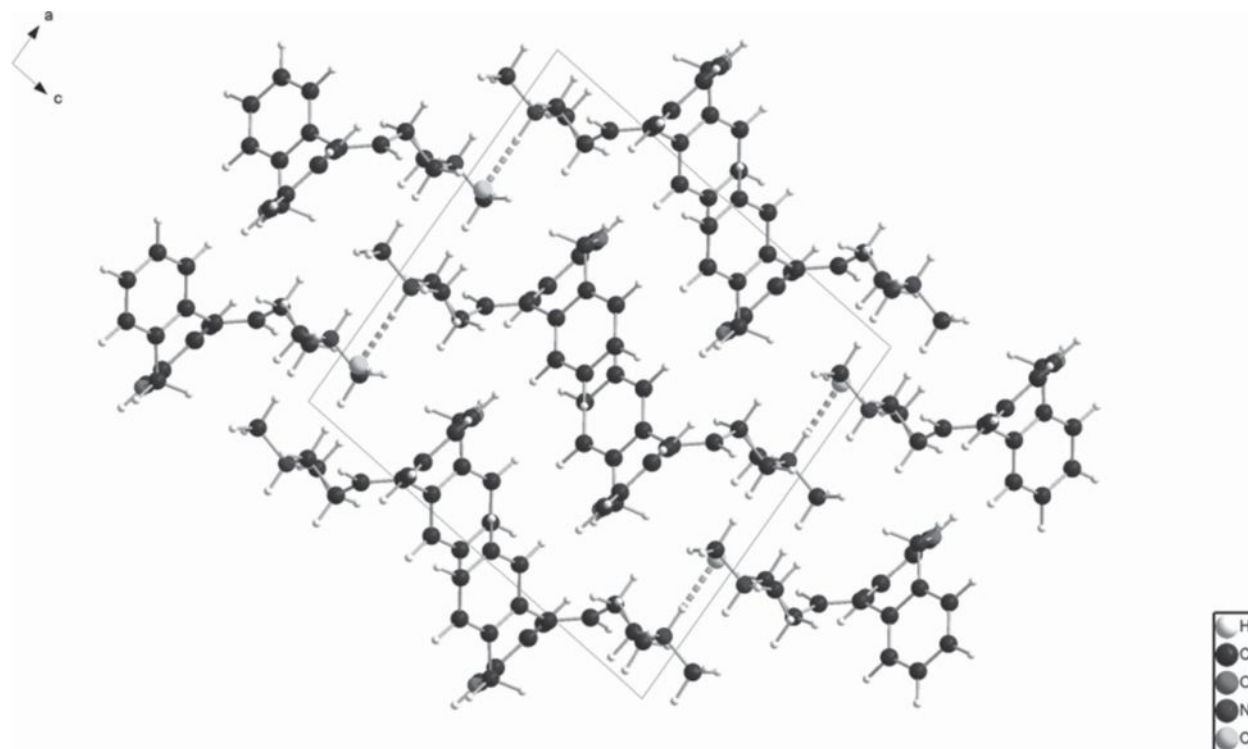
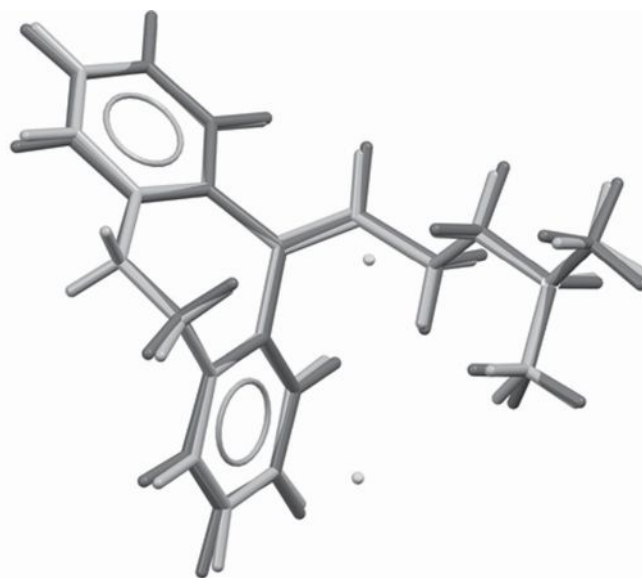


Figure 6. The crystal structure of doxepin hydrochloride, viewed down the *b*-axis.



Doxepin = green; YOVZEO = orange; rms delta = 0.084, max = 0.129

Figure 7. Comparison of the structure of doxepin hydrochloride (green) to that of amitriptyline hydrochloride (Klein *et al.*, 1994; YOVZEO; orange). The rms Cartesian displacement of the cations is 0.084 Å.

TABLE I. Hydrogen bonds (CRYSTAL14) in (*E*)-doxepin hydrochloride.

H-bond	D-H (Å)	H...A (Å)	D...A (Å)	D-H...A (°)	Overlap (<i>e</i>)
N34–H44...Cl43	1.058	1.977	3.030	172.7	0.118
C31–H33...Cl43	1.093	2.481	3.532	160.8	0.042
C39–H41...Cl43	1.092	2.579	3.634	162.2	0.040
C31–H32...Cl43	1.094	2.949	3.926	148.9	0.022
C35–H36...Cl43	1.090	2.877	3.847	148.3	0.021
C39–H42...Cl43	1.091	2.913	3.841	143.0	0.019
C35–H38...Cl43	1.090	2.896	3.831	144.0	0.018
C11–H13...Cl43	1.098	2.990	4.017	155.8	0.022
C28–H29...Cl43	1.097	3.109	3.817	122.9	0.010
C26–H27...Cl43	1.089	3.081	4.062	150.1	0.018

thus play a role in determining the observed solid-state conformation.

Analysis of the contributions to the total crystal energy using the Forcite module of Materials Studio (Dassault, 2019) suggests that bond, angle, and torsion distortion terms are significant in the intramolecular deformation energy, as might be expected for a fused ring system. The intermolecular energy is small and dominated by electrostatic attractions, which in this force-field-based analysis includes hydrogen bonds. The hydrogen bonds are better analyzed using the results of the DFT calculation.

Hydrogen bonds are prominent in the crystal structure (Table I). As expected, there is a strong discrete hydrogen bond between the protonated nitrogen N34 and the chloride anion. Perhaps less expected are the six C–H...Cl hydrogen bonds between the methyl groups and the chloride, as well as additional hydrogen bonds from methylene groups and the vinyl proton H27. Most of these interactions are captured by Mogul in its list of short contacts (Figure 8). The hydrogen bonds are important to determining the solid-state conformation of the cation.

The volume enclosed by the Hirshfeld surface (Figure 9; Hirshfeld, 1977; Turner *et al.*, 2017) is 431.69 Å³, 98.33% of 1/4 the unit cell volume. The molecules are thus not tightly packed. All of the significant close contacts (red in Figure 9) involve the hydrogen bonds. The volume/non-hydrogen atom is relatively large, at 19.9 Å³.

The Bravais–Friedel–Donnay–Harker (Bravais, 1866; Friedel, 1907; Donnay and Harker, 1937) morphology suggests that we might expect platy morphology for (*E*)-doxepin hydrochloride, with {001} as the principal faces. A second-order spherical harmonic model was included in the refinement. The texture index was 1.010, indicating that preferred orientation was not significant in this rotated capillary specimen. The powder pattern of (*E*)-doxepin hydrochloride from this synchrotron data set is included in the Powder Diffraction File™ 00-066-1613.

DEPOSITED DATA

The supplementary material for this article, which includes Crystallographic Information Framework (CIF) files

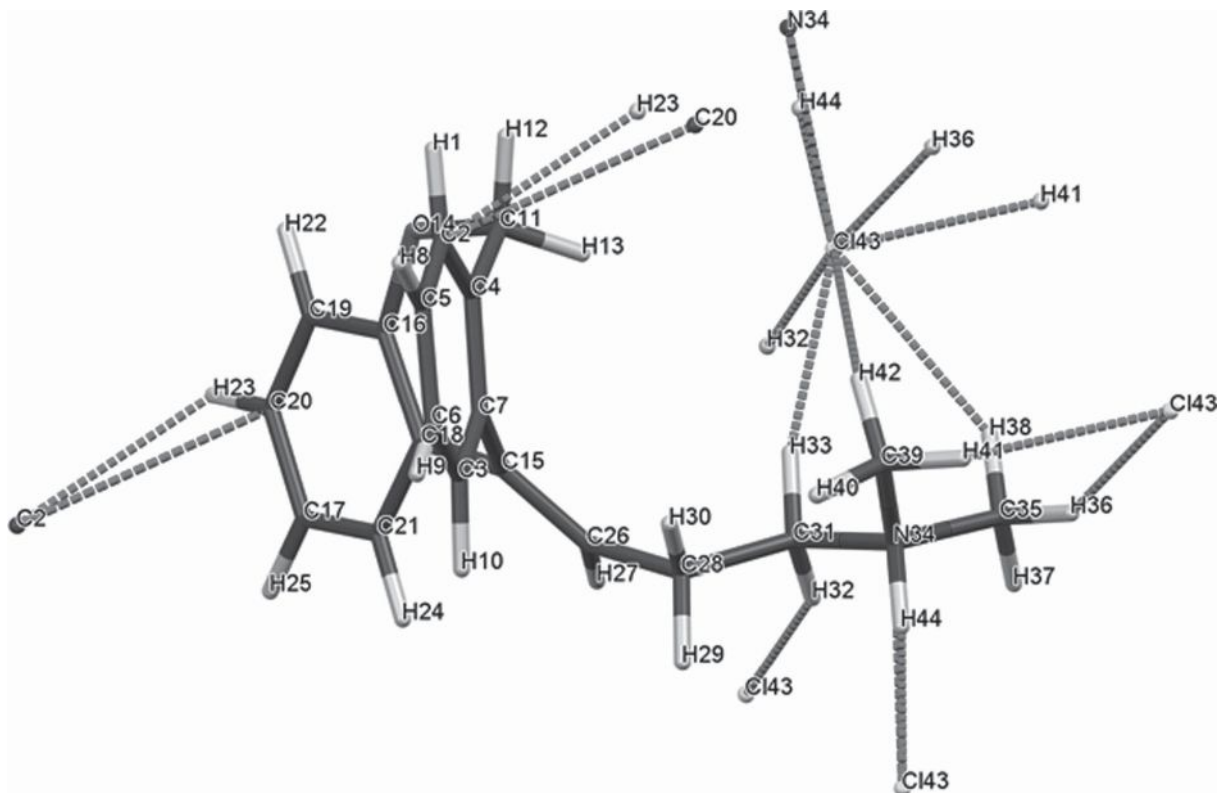


Figure 8. The weak C-H...Cl hydrogen bonds in doxepin hydrochloride.

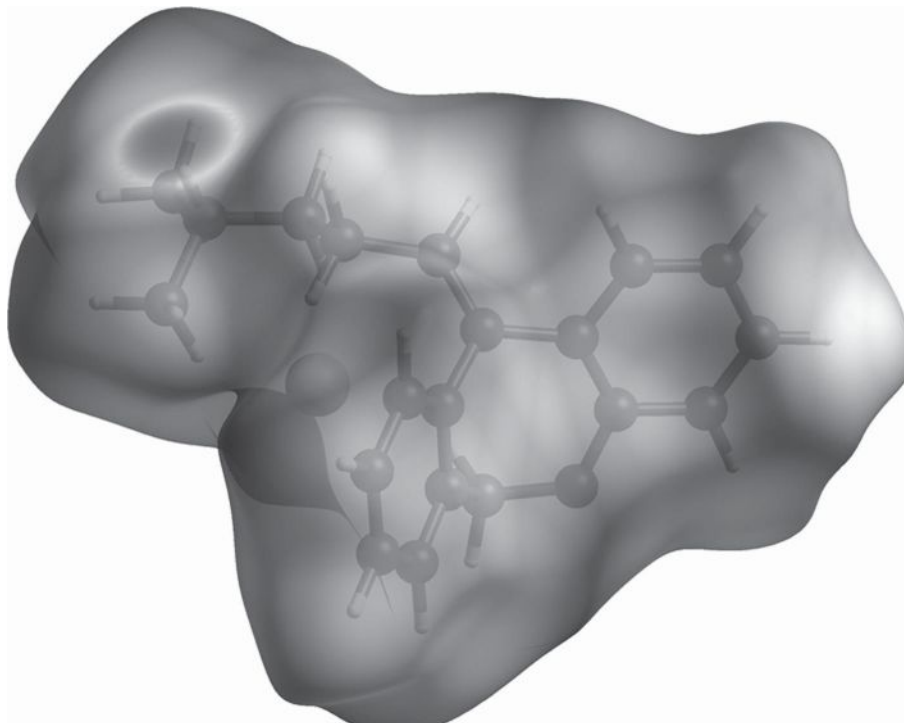


Figure 9. The Hirshfeld surface of doxepin hydrochloride. Intermolecular contacts longer than the sums of the van der Waals radii are colored blue, and contacts shorter than the sums of the radii are colored red. Contacts equal to the sums of radii are white.

containing the results of the Rietveld refinement (including the raw data) was deposited with the ICDD. The data can be requested at info@icdd.com.

ACKNOWLEDGEMENTS

Use of the Advanced Photon Source at Argonne National Laboratory was supported by the U.S. Department of Energy,

Office of Science, Office of Basic Energy Sciences, under Contract No. DE-AC02-06CH11357. This work was partially supported by the International Centre for Diffraction Data. We thank Lynn Ribaud and Saul Lapidus for their assistance in the data collection, and Andrey Rogachev for the use of computing resources at IIT.

CONFLICTS OF INTEREST

The authors have no conflicts of interest to declare.

- Altomare, A., Cuocci, C., Giacobazzo, C., Moliterni, A., Rizzi, R., Corriero, N., and Falcicchio, A. (2013). "EXPO2013: a kit of tools for phasing crystal structures from powder data," *J. Appl. Crystallogr.* **46**, 1231–1235.
- Bravais, A. (1866). *Etudes Cristallographiques* (Gauthier Villars, Paris).
- Bruno, I. J., Cole, J. C., Kessler, M., Luo, J., Motherwell, W. D. S., Purkis, L. H., Smith, B. R., Taylor, R., Cooper, R. I., Harris, S. E., and Orpen, A. G. (2004). "Retrieval of crystallographically-derived molecular geometry information," *J. Chem. Inf. Sci.* **44**, 2133–2144.
- Dassault Systèmes (2019). *Materials Studio 2019* (BIOVIA, San Diego, CA).
- DeCamp, W. (1982). Private communication; PDF entry 00-034-1704.
- Donnay, J. D. H. and Harker, D. (1937). "A new law of crystal morphology extending the law of Bravais," *Am. Mineral.* **22**, 446–447.
- Dovesi, R., Orlando, R., Erba, A., Zicovich-Wilson, C. M., Civalleri, B., Casassa, S., Maschio, L., Ferrabone, M., De La Pierre, M., D-Arco, P., Noël, Y., Causà, M., and Kirtman, B. (2014). "CRYSTAL14: a program for the ab initio investigation of crystalline solids," *Int. J. Quantum Chem.* **114**, 1287–1317.
- Friedel, G. (1907). "Etudes sur la loi de Bravais," *Bull. Soc. Fr. Mineral.* **30**, 326–455.
- Gates-Rector, S. and Blanton, T. (2019). "The Powder Diffraction File: a quality materials characterization database," *Powd. Diffr.* **39**, 352–360.
- Gatti, C., Saunders, V. R., and Roetti, C. (1994). "Crystal-field effects on the topological properties of the electron-density in molecular crystals - the case of urea," *J. Chem. Phys.* **101**, 10686–10696.
- Groom, C. R., Bruno, I. J., Lightfoot, M. P., and Ward, S. C. (2016). "The cambridge structural database," *Acta Crystallogr. B: Struct. Sci., Cryst. Eng. Mater.* **72**, 171–179.
- Haga, N. (1979). ICDD Grant-in-Aid; PDF entry 00-029-1697.
- Hirshfeld, F. L. (1977). "Bonded-atom fragments for describing molecular charge densities," *Theor. Chem. Acta* **44**, 129–138.
- Jin, Z. (2001). ICDD Grant-in-Aid; PDF entry 00-051-1920.
- Kaduk, J. A., Crowder, C. E., Zhong, K., Fawcett, T. G., and Suhomel, M. R. (2014). "Crystal structure of atomoxetine hydrochloride (Strattera), C₁₇H₂₂NOCl," *Powd. Diffr.* **29**, 269–273.
- Klein, C. L., Lear, J., O'Rourke, S., Williams, S., and Liang, L. (1994). "Crystal and molecular structures of tricyclic neuroleptics," *J. Pharm. Sci.* **83**, 1253–1256.
- Lee, P. L., Shu, D., Ramanathan, M., Preissner, C., Wang, J., Beno, M. A., Von Dreele, R. B., Ribaud, L., Kurtz, C., Antao, S. M., Jiao, X., and Toby, B. H. (2008). "A twelve-analyzer detector system for high-resolution powder diffraction," *J. Synch. Rad.* **15**, 427–432.
- Macrae, C. F., Sovago, I., Cottrell, S. J., Galek, P. T. A., McCabe, P., Pidcock, E., Platings, M., Shields, G. P., Stevens, J. S., Towler, M., and Wood, P. A. (2020). "Mercury 4.0: from visualization to design and prediction," *J. Appl. Crystallogr.* **53**, 226–235.
- Panda, R. (2011). "Study of polymorphism in doxepin hydrochloride," Ph.D. Dissertation, Rajiv Gandhi University of Health Sciences. Available at: <http://localhost:8080/xmlui/handle/123456789/5300>.
- Peintinger, M. F., Vilela Oliveira, D., and Bredow, T. (2013). "Consistent Gaussian basis sets of triple-zeta valence with polarization quality for solid-state calculations," *J. Comput. Chem.* **34**, 451–459.
- Sykes, R. A., McCabe, P., Allen, F. H., Battle, G. M., Bruno, I. J., and Wood, P. A. (2011). "New software for statistical analysis of Cambridge Structural Database data," *J. Appl. Crystallogr.* **44**, 882–886.
- Toby, B. H. and Von Dreele, R. B. (2013). "GSAS II: the genesis of a modern open source all purpose crystallography software package," *J. Appl. Crystallogr.* **46**, 544–549.
- Turner, M. J., McKinnon, J. J., Wolff, S. K., Grimwood, D. J., Spackman, P. R., Jayatilaka, D., and Spackman, M. A. (2017). *CrystalExplorer17* (University of Western Australia). Available at: <http://hirshfeldsurface.net>.
- van de Streek, J., and Neumann, M. A. (2014). "Validation of molecular crystal structures from powder diffraction data with dispersion-corrected density functional theory (DFT-D)," *Acta Crystallogr. B: Struct. Sci., Cryst. Eng. Mater.* **70**, 1020–1032.
- Wang, J., Toby, B. H., Lee, P. L., Ribaud, L., Antao, S. M., Kurtz, C., Ramanathan, M., Von Dreele, R. B., and Beno, M. A. (2008). "A dedicated powder diffraction beamline at the advanced photon source: commissioning and early operational results," *Rev. Sci. Instr.* **79**, 085105.
- Wavefunction, Inc. (2018). Spartan '18 Version 1.2.0, Wavefunction Inc., 18401 Von Karman Ave., Suite 370, Irvine, CA 92612.